ORIGINAL PAPER

Biodegradable Membrane with High Porosity and Hollow Structure Obtained via Electrospinning for Oil Spill Clean-up Application

Roberto Scaffaro[1] · Emmanuel Fortunato Gulino[1] · Maria Clara Citarrella[1]

Abstract

The use of biodegradable polymers for the production of membranes to be used in wastewater treatment has attracted increasing interest considering the possibility of reducing the risk of second pollution. In this work, porous fibrous membranes based on polylactic acid and polyethylene oxide (PEO) blends were prepared. The solutions were electrospun using two approaches: (i) conventional coaxial electrospinning followed by leaching treatment (double-step, DS); (ii) coaxial wet electrospinning with in situ leaching (single-step, SS). By varying PEO type and processing method it was possible to control membranes structure and porosity. DS leaching treatment lead to surface porosity (i.e. shell leaching), while SS allowed obtaining hollow and porous fibers (i.e. with shell and core leaching). Process, properties and structure relationships of devices were analysed trough rheological, morphological, mechanical and surface characterizations. Furthermore, the influence of the different porous structures on oil sorption capacity and reusability of the membranes was evaluated. Results reveal that different porosities lead to a variation in membranes mechanical performance, in their wettability and, consequently, in their oil spill cleanup capacity. Membranes obtained with SS displayed higher performance in oil removal if compared to the DS ones, due to their hollow structure and higher surface area.

Graphical Abstract

Abbreviations

Ac	Acetone
CF	Chloroform
DS	Double-step
E	Elastic modulus
EB	Elongation at break
ES	Electrospinning

Extended author information available on the last page of the article

PEO-A　　Polyethylene oxide Mw 100 kDa
PEO-B　　Polyethylene oxide Mw 600 kDa
PLA　　　Polylactic acid
q　　　　 Absorption capacity
SEM　　　Scanning electron microscope
SS　　　　Single-step
TS　　　　Tensile strength
W　　　　 Wet
WCA　　 Water contact angle

Introduction

Water pollution is currently one of the major global problem [1–4]. To solve this issue the production of fibrous membranes based on biodegradable polymers, able to absorb oil, is of great interest as it would allow to solve the problem of secondary pollution [5]. The ability of absorbing oil is strictly related to pore morphologies of the membranes [1, 6]. In general, in fact, in biopolymeric fibrous devices, high porosity is definitely a key factor for successful applications such as: controlled drug release [7–9], pollutant removal [10–14], biomedical items [15–18]. High porosity and, consequently, high surface area, in fact, are essential to optimize their final performance. Electrospinning (ES), together with its variants, is one of the most reported techniques for the obtainment of nanofibers [19]. In ES, the polymeric solution is loaded into a syringe pump with a needle tip (the spinneret) and due to the supply high voltage power is charged forming polymeric fibers. Moreover, ES is a very versatile technique that allow to obtain complex nanofibers structures by changing spinneret and (or) collector design. Recently, coaxial electrospinning process has been used to fabricate new nanofibers with core–shell structure [20]. In this latter case, the spinneret is composed by two concentric needles connected with two different syringe pumps. By appropriately selecting the two different polymeric solutions, it is possible to obtain nanofiber with particularly complex structures, including hollow fibers [20].

Over the last years, the traditional solid collector has been replaced with a liquid one in several studies in order to fabricated hierarchical structure [21]; functionalize [22] or crosslink [23] the nanofibers; obtain hollow fibers by removing the core component [24].

In polymeric based systems, porosity is commonly obtained either by a main forming process followed by post processing treatments or by the combination of several processes in one, two or more steps [6, 14, 25]. Concerning the first case, post processing leaching is one of the most effective methods to obtain devices with high surface area [26–28]. In the leaching method, after dissolving the polymer (that is going to form the matrix) and a porogen

(usually another polymer, salt or other additives) in a common solvent, the obtained solution is electrospun and, subsequently, the prepared membrane is submerged in a solution, solvent of the porogen and non-solvent of the matrix, in order to remove the porogen and obtain porous nanofibers. Zhang et al. [29], for example, employed leaching method to produce porous nanofibers by selectively removing the water-soluble component of gelatine. Ning et al. [30], fabricated porous Polyvinylidene fluoride (PVDF) nanofibers by leaching method using polyethylene oxide (PEO) as porogen. Moreover, an environmental friendly technology, based on the combination of melt mixing and leaching of salt in water, was developed to prepare porous three-layer scaffolds [12, 31–33]. Post processing treatments, however, are characterized by some negative aspects. Often, in fact, beyond they require the use of chemicals that could be toxic to human health and environment they definitely increase the whole processing time which implies an increase of production costs of the final device [34]. A possible strategy, to overcome these limits, is to combine multiple processes or treatments to get forming and pores generation by a single step process. Polyacrylonitrile (PAN) fibers, for example, were prepared in one-step by exploiting phase separation during electrospinning process [35]. Moreover, highly porous fibrous systems can be also obtained by inducing phase separation in systems with different evaporation rates, formulated using appropriate solvent/non-solvent couples of the polymer [36, 37]. Porosity is a key factor in mass transfer (release/removal) applications [7, 38, 39].

Polymers originated from biomass have recently gained attention due to oil resources exhaustion and environmental pollution. Polylactic acid (PLA) is a plant-based polymer used in many applications because of its interesting physical properties, renewability and biodegradability. Polyethylene oxide (PEO) is a polymer prepared by polymerization of ethylene oxide characterized by a high solubility in water and non-toxicity. It is often added in mixture with other polymers to increase their hydrophilicity, to enhance its processability or used as a sacrificial phase to obtain highly porous structures after its leaching in water [40].

In this work, biodegradable porous fibrous PLA/PEO membranes were produced by two different processing methods: a conventional coaxial electrospinning with a subsequent leaching treatment (double-step, DS) and a coaxial wet electrospinning with in situ leaching treatment (single-step, SS). PLA:PEO blends, in different ratio and using PEO with two different M_w, were electrospun/leached following both processing paths. The relationships between process, properties and structure of the obtained devices were analysed through rheological, morphological, mechanical and surface characterizations. Furthermore, the influence of the different porous structures (obtained both for single-step and

double-step method) on oil absorption capacity and reusability of the membranes was evaluated.

Materials and Method

Materials

Polylactic acid 2003D Mw 98 kDa (PLA), was purchased from Nature Works. Polyethylene oxide Mw 100 kDa (PEO-A), Polyethylene oxide Mw 600 kDa (PEO-B), acetone (Ac), chloroform (CF) and distilled water were purchased from Sigma Aldrich. All the reactants were ACS grade (purity > 99%) and were used as received.

Standard oily motor 10W–40 (density = 0.87 g/cm^3 kinematic viscosity = 97.7 mm^2/s at 40 °C) was supplied by Total S.A. Chemical composition of oil consists in hydrocarbons between 18 and 34 carbon atoms per molecule. Commercial food grade olive oil and sunflower oil were used. The three oils were also tested in their exhausted version, i.e. at their end-of-life.

Preparation of Polymeric Solution

PLA, PEO-A and PEO-B solutions ware prepared by dissolving the respective required amount of polymer in a CF/Ac mixture (2:1 ratio) under magnetic stirring at 25 °C overnight. A preliminary study of starting solutions and blends were carried out in order to verify their processability and detail are reported in Supporting Information. PLA 10 wt%; PEO-A 10 wt% and PEO-B 5 wt% were selected for further investigations and from here on we will refer to these concentrations by using acronyms PLA, PEO-A and PEO-B. As regards the shell polymeric solutions, PLA was mixed with PEO-A or PEO-B at different relative ratio and PLA/PEO-A and PLA/PEO-B obtained blends were stirring overnight in order to obtain a homogeneous solution. The compositions of blends here produced are listed in Table 1. PEO-A (10 wt% in CF/Ac 2:1 mixture) was used as core solution for PLA/PEO-A systems and PEO-B (5 wt% in CF/Ac 2:1 mixture) for PLA/PEO-B ones.

Table 1 Composition of shell PLA/PEO-A and PLA/PEO-B blends

Sample code	PLA (wt %)	PEO-A (wt %)	PEO-B (wt %)
PLA/PEO-A25	75	25	0
PLA/PEO-A50	50	50	0
PLA/PEO-A75	25	75	0
PLA/PEO-B25	75	0	25
PLA/PEO-B50	50	0	50
PLA/PEO-B75	25	0	75

Preparation of Porous Membranes via Double-Step (DS) Processing

Membranes were prepared by using a conventional electrospinning equipment consisting in a syringe pump and a high voltage power supply (Linari Engineering-Biomedical Division, Pisa, Italy). The polymeric solutions were filled in a 10 mL glass syringe equipped with coaxial needles manufactured in AISI 316 stainless steel. The outer needle was attached to the syringe pump containing the shell solution (PLA/PEO-A or PLA/PEO-B) and the inner was connected to a pump having, in the core solution (PEO-A or PEO-B respectively). The process was performed using the following parameters: supplied high voltage 15 kV; flow rate, 1.5 mL/h; distance between coaxial needles tip and collector, 12 cm; temperature, 25 °C; and relative humidity, 40%. The solutions were electrospun on a grounded collector wrapped in aluminium foil for 1 h. Aiming to verify if the gravity could affect the electrospinning process, preliminary DS membranes were prepared with both horizontal and vertical assembly of the electrospinning set-up. Any statistically significant differences have been noted between the membranes obtained with the two set-ups from both morphological and mechanical point of view. Considering that, we decided to keep the horizontal arrangement of the set-up for convenience.

In order to remove the sacrificial polymer (PEO-A or PEO-B) from the membranes (~20 mm in diameter, about 100 μm in thickness), they were submerged in 20 mL of distilled water at 25 °C for 30 min at 50 rpm stirring. After immersion, the membranes were dried overnight in a vacuum oven. A summary schematic of the process is depicted in Fig. 1a.

Preparation of Porous Membranes via Single-Step (SS) Processing

Membranes were also prepared in SS processing using the same electrospinning apparatus, appropriately modified, with the same processing parameters reported above. More in detail, as depicted in Fig. 1b, the polymeric solutions were filled in a 10 mL glass syringe equipped with coaxial needles that was placed on a vertically arranged syringe pump. The solutions were then electrospun for 1 h on a liquid-bath grounded collector (known as wet collector) wrapped in aluminium foil at the bottom of the vessel. The wet collector (previously equipped with a magnetic stirrer) and was placed onto a stirrer set at 50 rpm in order to promote fibers dispersion in the liquid bath. A photographical image of the set-up is provided in Fig. S1. The use of the wet grounded collector allowed the fibers to be submerged in water contextually to their formation [21, 24, 41] aiming to efficiently remove the
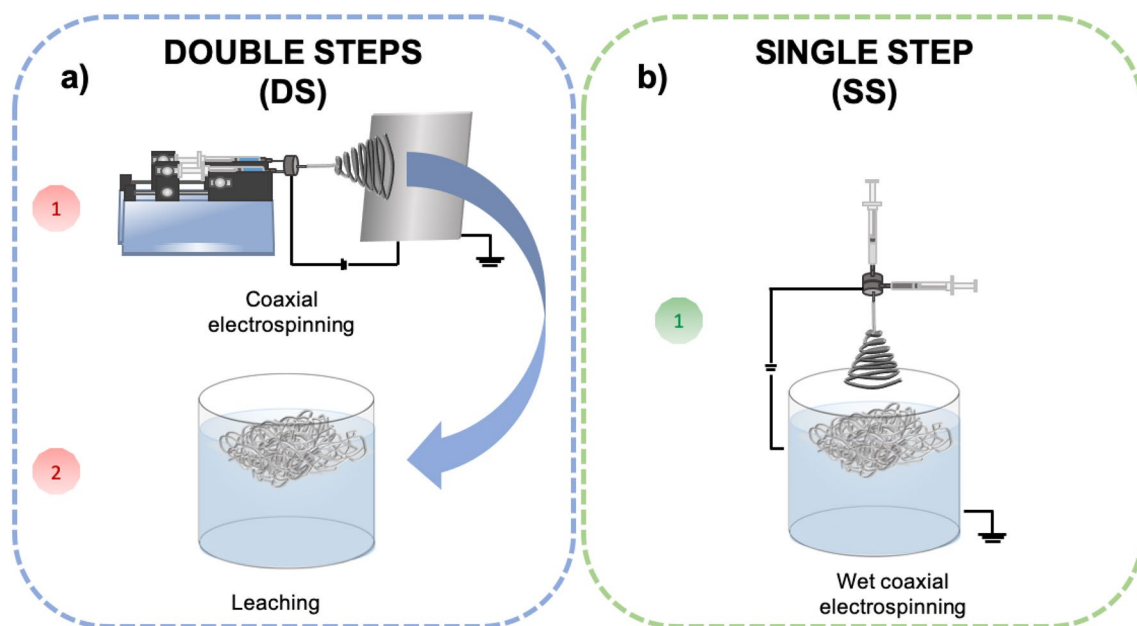
Fig. 1 Two-step preparation of dual porous membrane via coaxial electrospinning (**a**), One-step preparation of dual porous membranes via coaxial wet electrospinning (**b**)

sacrificial polymer in situ (single step). After processing, the membranes were dried in a vacuum oven overnight.

Rheological Characterization

Rheological properties of polymeric solutions were tested by rotational rheometer (ARES-G2). A 25 mm parallel-plate geometry was used and all tests were performed at 25 °C. Oscillatory frequency sweep tests were performed at a constant stress of 1 Pa with an increase of angular frequency from 1 to 100 rad/s. This frequency range was considered since measurements below 1 rad/s reported unusable data and only above 1 rad/s significant data was obtained.

Morphological Characterization

The morphology of the nanofibers was observed by using a scanning electron microscope (SEM, Phenom ProX, Phenom-World, The Netherlands) with optical magnification range of 20–135x, electron magnification range of 80–130,000×, maximal digital zoom of 12×, acceleration voltages of 15 kV. The microscope is equipped with a temperature controlled (25 °C) sample holder. The samples were positioned on an aluminium stub using an adhesive carbon tape. Fibers diameter size distribution was measured using Image J software, equipped with Diameter J plugin. This plugin is able to analyse an image and find the diameter of nanofibers at every pixel along a fibers axis. The software produces a histogram of these diameters and summary statistics such as mean fibers diameter. The diameters of 100

fibers for each SEM image were measurement. Each measurement was performed in triplicate.

FT-IR/ATR Analysis

Chemical and structural characterization of samples surfaces were assessed by FT-IR/ATR analysis, carried out by using a Perkin-Elmer FT-IR/NIR Spectrum 400 spectrophotometer. The absorbance spectra were recorded in the wavenumber range 4000–400 cm^{-1}.

Water Contact Angle (WCA) Measurements

Surface wettability of the fiber mats were measured by an FTA 1000 (First Ten Ångstroms, UK) instrument. More in detail, 4 μL of deionized water were dropped onto fiber mats. Images of the water droplet were taken at a time of 10 s. At least five spots of each fiber mat were tested and the average value was taken.

Mechanical Properties

The mechanical performance of the membranes was investigated by carrying out tensile test on a laboratory dynamometer (Instron model 3365, UK) equipped with a 1 kN load cell. Tests were performed on rectangular shaped specimens (10×90 mm) cut off from the membranes. A double crosshead speed was used: 1 mm min^{-1} for 2 min and 50 mm min^{-1} until fracture occurred. The grip distance was 30 mm, whereas the sample thickness was measured before

each test. Six specimens were tested for each sample and the outcomes of elastic modulus (E), tensile strength (TS), and elongation at break (EB), have been reported as average values ± standard deviations.

Oil Spill Clean-up Capacity

The absorption capacity of fibrous membranes were evaluated by placing about 0.15 g of electrospun mat in a beaker filled with 25 g of water and 50 g of oil and taken out instantaneously. The excess oil present on the fibers, not really adsorbed by the membrane, was drained out for 30 s. All the experiments were carried out in triplicate.

The absorption capacity (q) can be calculated by the equation:

$$q(g/g) = \frac{W_a - W_i}{W_i}$$

where W_i is the initial weight of the membrane and W_a is the weight of the membrane after oil absorption.

Reusability

Oil absorption ability of the electrospun membranes was monitored for five cycles in order to evaluate their reusability. After each absorption cycle the membranes were squeezed with padding paper, washed with ethanol aiming to remove the absorbed oil and let it air dry. After each cleaning step the membranes were reweighted and this latter weight was taken as a new dry reference for absorption capacity measurement. Moreover, q variation was considered in order to evaluated reusability of the membranes.

Statistical Analysis

Statistical analysis was performed on obtained data through unpaired Student t-test, using GraphPad Prism 9. Differences between two sets of data were considered statistically significant when the p-value obtained was lower than 0.05.

Results and Discussion

Rheological Characterization of the Polymeric Solution

After a preliminary investigation (see Supporting Information), PEO-B 5 wt% and PEO-A 10 wt% have been chosen for further preparation. Different concentration of PEO-A and PEO-B in PLA blend may play a key role to obtain the desired porous structure. To investigate about processing

behavior of PLA/PEO blends, rheological tests have been performed and the results are reported in Fig. 2a, b.

In general, all systems showed a pronounced non-Newtonian behavior in the whole frequencies range and for both PEOs, at any PLA/PEO ratio. Moreover, all the blends displayed higher viscosity if compared to neat PLA. As regards PLA/PEO-A blends, in Fig. 2a it can be observed that their rheological behavior is substantially dominated by PLA up to 50 wt% PEO. Differently, PLA/PEO-A75 viscosity curve, similarly to that of neat PEO-A, presents remarkable non-Newtonianism with an ensuing more pronounced shear thinning at higher frequencies, similarly to PEO-A. Regarding PLA/PEO-B blends, presented in Fig. 2b, any dependence on PLA up to 50wt% PEO can be noted. Contrariwise, the progressive PEO-B addition induces a gradual increase in the viscosity of the solutions [40]. The non-Newtonian behavior is preserved for all PLA/PEO-B blends in the whole frequencies range.

Considering that in our case the shear rate was estimated as about 4 1/s and that consequently it was found (in the preliminary investigation reported in Supporting Information) that the effective operating viscosity range to achieve good electrospun structures is therefore about 10^2–$5*10^3$ Pa*s, it is possible to observe that all PLA/PEO-A and PLA/PEO-B
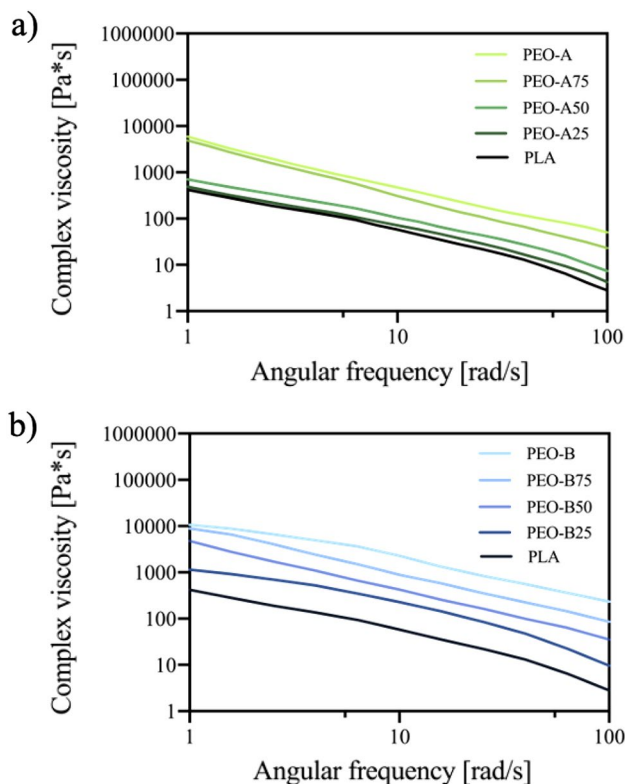
Fig. 2 Rheological curves of PLA/PEO-A (**a**), PLA/PEO-B (**b**) blends solutions at different PLA/PEO ratio

blend fall within this range. This outcome suggested the potential electrospinnability of all the PLA/PEO blends.

Morphological Characterization of the Fibrous Membranes

The morphology of PLA/PEO-A and PLA/PEO-B electrospun mats together with corresponding fibers diameters distribution diagrams are shown in Fig. 3.

It is well known that electrospinning of high viscosity solutions leads to fibers with large and irregular diameters

[42]. In accordance with the scientific literature, PLA/PEO-A25 and PLA/PEO-B25 membranes (Fig. 3a, b respectively) resulted in randomly oriented continuous fibers with rough and large surface and bead-free morphology. Moreover, they both displayed unimodal size distributions, whose mean values of 1 and 1.2 μm respectively (Fig. 3c). PLA/PEO-A50 and PLA/PEO-B50 membranes (Fig. 3d, e respectively) displayed fibers diameter average values of 1.2 μm and 1.23 μm respectively (not statistically significant; Fig. 3f). Also in these cases, a unimodal size distribution can be noted (Fig. 3f). Moreover, it is possible to observe the presence
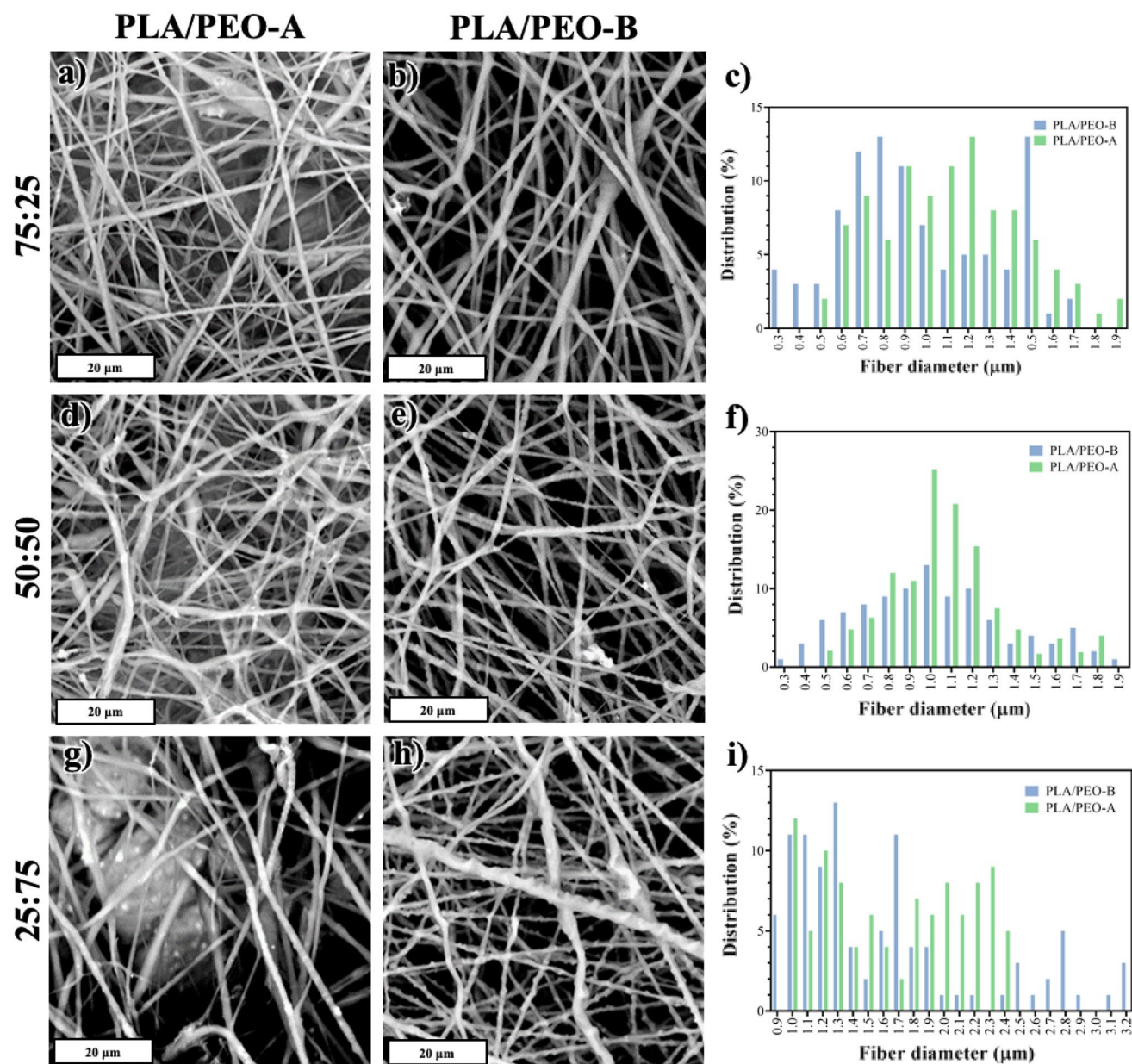

Fig. 3 SEM micrographs of PLA/PEO-A25 (**a**), PLA/PEO-A50 (**b**), PLA/PEO-A75 (**d**), PLA/PEO-B25 (**e**), PLA/PEO-B50 (**g**) and PLA/PEO-B75 (**h**) electrospun membranes and corresponding fibers diameters distribution diagrams (**c, f, i**)

of two distinct phases along the fibers, probably identifiable with PEO agglomerations can be identify along PLA fibers (see for instance red line in Fig. 3e). On the contrary, PLA/PEO-A75 and PLA/PEO-B75 (Fig. 3g, h respectively) showed a multimodal size distribution with maxima and mean values of 2 and 1.9 respectively (Fig. 3i). Furthermore, the presence of PEO agglomerations along the fibers are even more evident in these cases. In general, the presence of PEO agglomerations is more evident in PEO-B containing systems if compared to PEO-A ones, for each PEO concentrations. This behavior can be reasonably explained considering that PEO-A and PEO-B have quite different molecular weights. PEO-A (100 kDa), in fact, is likely characterized by higher miscibility in PLA if compared to PEO-B (600 kDa) as reported elsewhere for similar systems [40, 43]. Lower miscibility of PEO-B reasonably lead to the formation of larger PEO aggregates along fibers surface (see, for example, red arrow in Fig. 3h). In order to ensure a better readability, fibers diameters distribution diagrams have been also provided in Figure S2-4 in a larger version.

The presence of different concentrations of PEO-A or PEO-B plays a key role in obtaining membranes with different porosity. Both PEO-A and PEO-B, in fact, are totally soluble in water and for this reason they were chosen as sacrificial phases. As regards DS process, by submerging the obtained membranes in water, leaching of the PEO phase was performed and a higher porosity in electrospun membranes was verified by SEM, as shown in Fig. 4.

After leaching, PLA/PEO-A25L (Fig. 4a) showed a quite stable structure with a good retention of fiber morphology and the presence of pores along fibers surface. On the contrary, PLA/PEO-B25L membrane (Fig. 4b) exhibited porous and non-homogeneous fibers with coalescence between some of them. When 50% of PEO is added (Fig. 4d, e), more marked differences can be observed between membranes before and after leaching. In particular, PLA/PEO-A50L (Fig. 4d) showed an alteration of fibrous structure with starting coalescence between fibers. On the contrary, PLA/PEO-B50L (Fig. 4e) showed a significant alteration of fibers architecture with a bad retention of fiber morphology. More in detail, fibers appear flattened and non-homogeneous reasonably due to poor miscibility of PEO-B in PLA phase. In fact, when 50% of PEO-B is leached, fibers collapse due to lack of support of insoluble phase (PLA) [40]. This behavior does not occur in the presence of PEO-A. Its better miscibility, if compared to PEO-B one, in fact, allows preserving fibers structure during leaching. Accordingly, in PLA/PEO-A75L (Fig. 4g) only a partial collapse of the fibers can be noted while PLA/PEO-B75L (Fig. 4h) showed a totally collapsed fibrous structure and no fibers can be observed. In order to ensure a better readability, fibers diameters distribution diagrams have been also provided in Figure S5 and S6 in a larger version.

Considering the good fibers retention after leaching of PLA/PEO-A25 and PLA/PEO-B25, the corresponding solutions were selected to be processed by adopting single step process. The use of the wet collector (SS) lead to different morphological structure due to in situ leaching occurrence. In Fig. 5 SEM micrographs and schematic description of leaching mechanism of PLA/PEO-A25W and PLA/PEO-B25W membrane are shown. PLA/PEO-A25W membrane (Figs. 5a, b, 6a) shows a quite stable structure with a good retention of fiber morphology and the presence of nano-porous and hollow fibers (Fig. 5f). Moreover, multimodal size distribution can be noted (Fig. 5e). PLA/PEO-B25W membrane (Fig. 5c, d) shows micro-porous and hollow fibers, however a less stable and homogeneous fibrous structure with a micro-porous fibers can be observed (Fig. 6f). Also in this case, a multimodal size distribution can be noted (Fig. 5g). Furthermore, fibers opening occurs (see Fig. 5h and, for example, arrow in Fig. 5c).

This behavior could be reasonably attributed to the presence of large agglomerations of PEO-B in the shell surface due to its poor miscibility in PLA [44]. In particular, when the fibers were projected to the wet collector, during electrospinning, sudden dissolution of PEO-B occurs inducing fiber opening with a peculiar morphology, showing a contextual intense leaching of core and shell of the fiber with pores widely distributed in both areas of the fiber, in some cases forming deep superficial furrows likely due to intense superficial leaching. This can be explained considering that PEO-B tends to form large aggregates that will turn in larger pores once leached.

Figure 7 shows a modelization of the leaching process in the two cases, based on the obtained results. As regards DS, Fig. 7a, post-processing leaching treatment occur in fibers with a stabilized structure without residual solvent. Consequently, 30 min of leaching is evidently not enough to grant complete core leaching. On the other hand, for SS, Fig. 7b, leaching and electrospinning occur simultaneously. During spinning, prior to fibers deposition in the wet collector, part of the solvent could remain inside the fibers. Therefore, the presence of non-stabilized fibers, containing residual solvent, promoted penetration of the leaching agent into the core. The two proposed mechanism are in full agreement with the observed morphologies in both cases.

FT-IR/ATR Analysis

In order to get further confirmations about leaching modelization in DS and SS, ATR-FTIR measurements were carried out on neat PLA, PLA/PEO-A and PLA/PEO-B blends mats before and after leaching. FTIR analysis was performed also on PLA/PEO-A25W and PLA/PEO-B25W membranes. The related FTIR spectra are shown in Fig. 8 and the relevant characteristic peaks are resumed in Table 2. PLA revealed
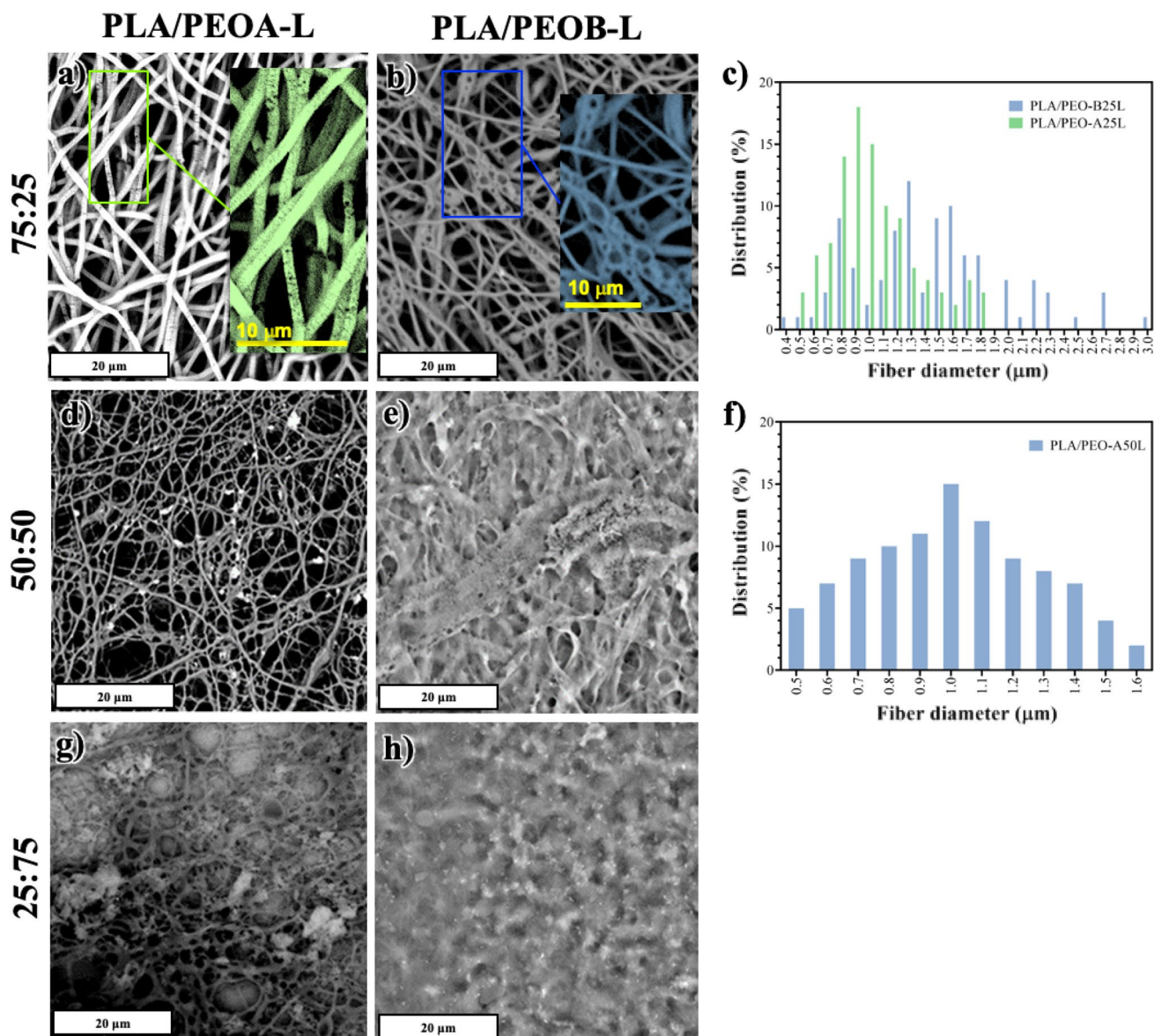
Fig. 4 SEM micrographs of PLA/PEO-A25L (**a**), PLA/PEO-B25L (**b**), PLA/PEO-A50L (**d**), PLA/PEO-B50L (**e**), PLA/PEO-A75L (**g**), and PLA/PEO-B75L (**h**) electrospun membranes and corresponding fibers diameters distribution diagrams (**c**, **f**)

a neat band at 1759 cm^{-1} (–C = O band referable to PLA carbonyl groups) [45, 46]. As expected, PLA/PEO-A and PLA/PEO-B blends show bands typical of both PLA and PEO-A or PEO-B. In particular, it could be noticed a band at 1344 cm^{-1} (CH$_2$), a peak at 1150 cm^{-1} (related to the C–O–C stretching vibration of PEO) and CH stretching mode at 2891 cm^{-1} in PEO-A and PEO-B spectra [47–49]. The same bands also appeared in PLA/PEOs blends confirming the correct incorporation of PEOs in the nanofibrous membranes. It is also possible to observe that these bands increase in intensity upon increasing the PEO-A or PEO-B amount in the blends. On the contrary, it is possible to observe a band with decreasing intensity (1759 cm^{-1}

carbonyl group PLA) upon increasing the PEO-A amount in the blends [50]. However, this behavior cannot be noticed for PEO-B blends.

Spectroscopical analysis therefore confirms that PEOs have been removed by leaching process both in DS and in SS. Moreover, in this latter case the decreasing of the related bands is more pronounced, confirming the hypotheses that more intense leaching occurs during SS process.

Water Contact Angle (WCA) Measurements

The membranes obtained by the two methods, are formed by fibers with different architectures, also causing changes

Fig. 5 PLA/PEO-A25W and PLA/PEO-B25W SEM micrograph (**a**, **b** and **c**, **d** respectively), corresponding fibers diameters distribution diagrams (**e**, **g** respectively) and of scheme of leaching mechanism (**f**, **h** respectively)
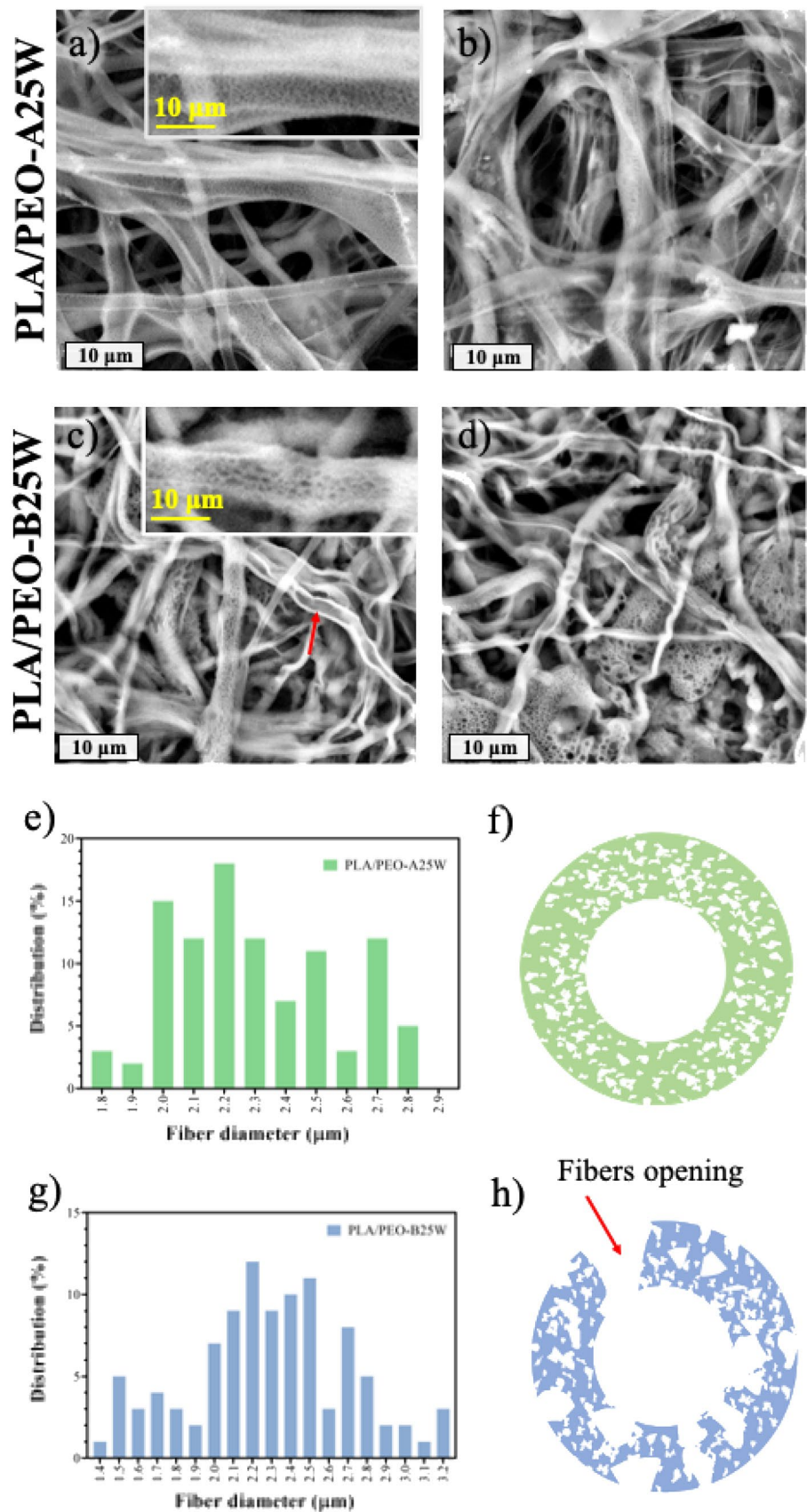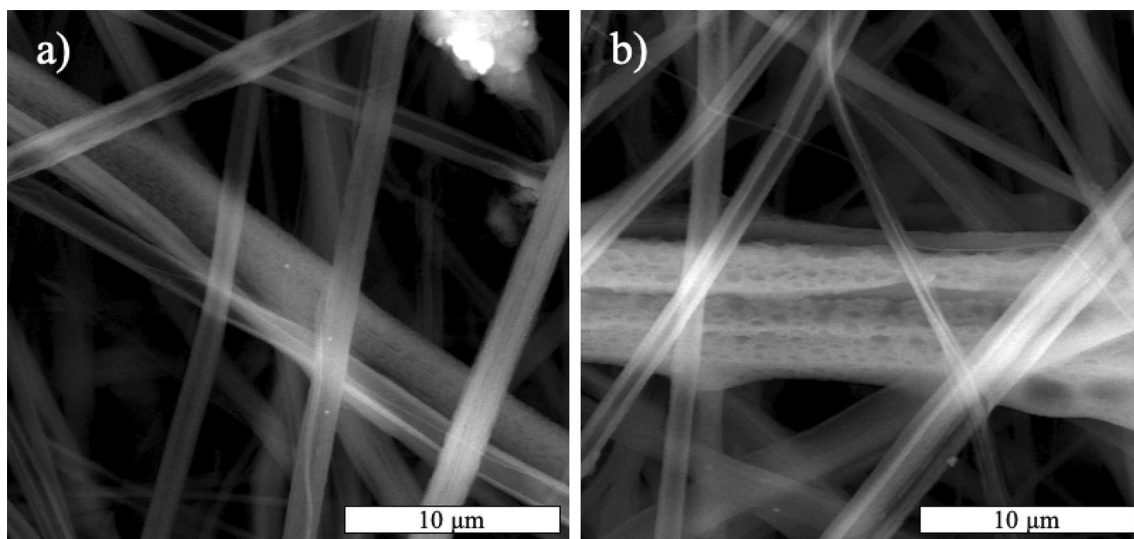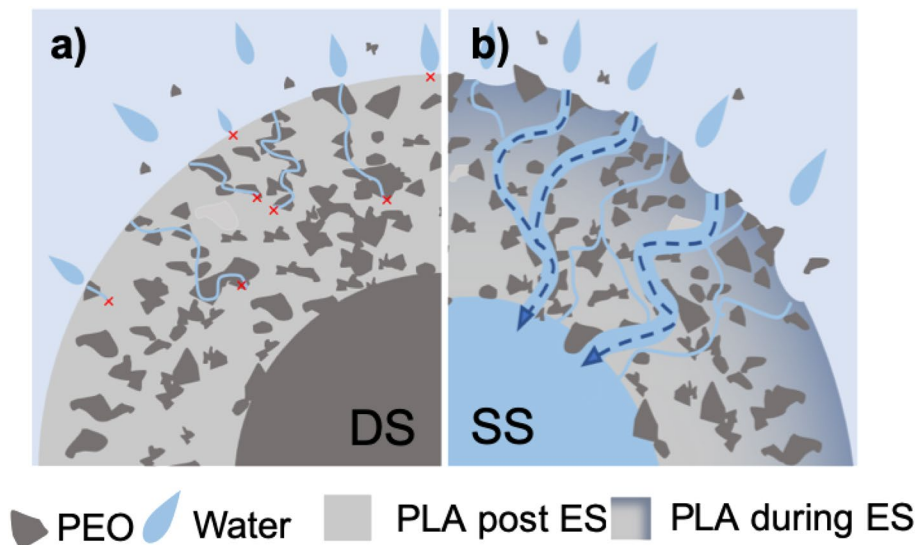
Fig. 6 PLA/PEO-A25W (**a**) and PLA/PEO-B25W (**b**) fibers SEM micrograph

Fig. 7 Schematic description of fibers leaching mechanism of shell leaching achieve with double-step method (**a**) and core and shell leaching achieve with single-step method (**b**)

in their wettability. In this view, water contact angle (WCA) tests have been performed on all the systems and results are reported in Fig. 9.

PLA showed a hydrophobic behavior with a WCA of 103° in accordance with the scientific literature [51, 52]. Non-leached systems containing PEO-A show higher WCA if compared to the PEO-B ones (Fig. 9). This behavior, according to the morphological characterization, could be explained by considering the presence of larger PEO agglomerations along the fibers in PLA/PEO-B blends if compared to PLA/PEO-A ones before the leaching step. WCA value of leached systems surprisingly showed an increase in wettability if compared to the non-leached ones. Moreover, this increase is even more evident for PLA/

PEO-A25W and PLA/PEO-B25W. This behavior, according to the morphological characterization, could be explained by considering the increase in porosity of the leached membranes: the presence of large pore and the achievement of a hollow structure in the fibers, induced by in situ PEO leaching, lead to the obtainment of membranes with long interconnected pores [43]. In fact, despite results seems to not match Wenzel equation, is necessary to consider that the hollow structure and the interconnected pores are responsible of liquid capillary transport through the membranes thus leading to peculiar fibers architecture and consequent lower WCA values [53].

Wenzel's equation state that WCA value should decrease as roughness increases. However, it is known in the scientific
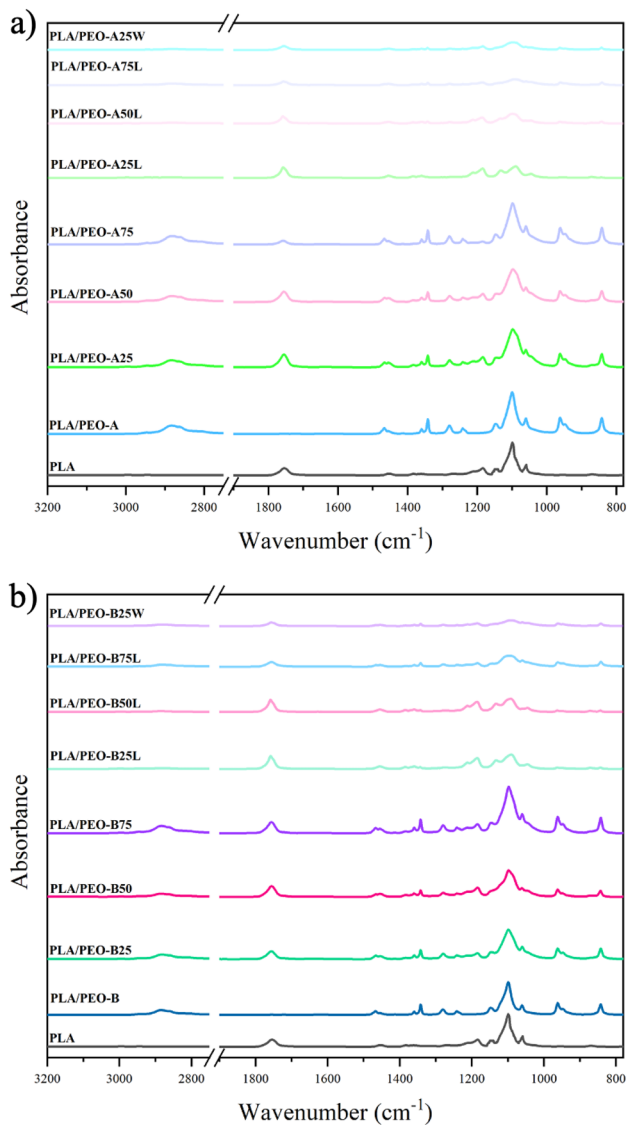
Fig. 8 ATR-FTIR measurements carried out on neat PLA, PLA/PEO-A, PLA/PEO-B blends mats before and after leaching and PLA/PEO-A25W, PLA/PEO-B25W
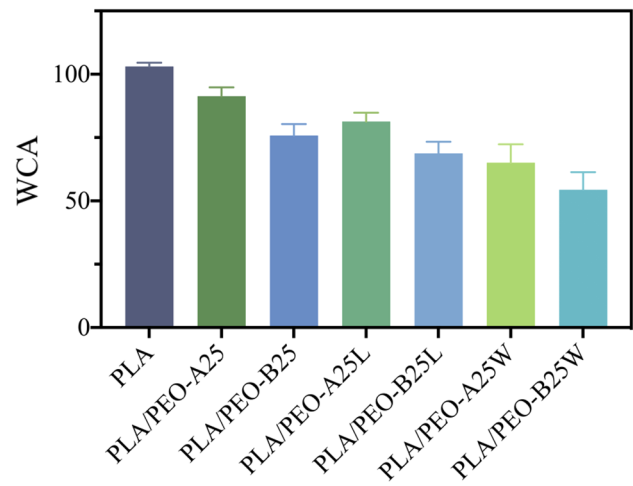

Fig. 9 WCA values of neat PLA, PLA/PEO-A25, PLA/PEO-B25, PLA/PEO-A25L, PLA/PEO-B25L, PLA/PEO-A25W and PLA/PEO-B25W membranes

literature that, even though roughness increases, the presence of long interconnected channel in the membrane leads to an increase in WCA value instead of decrease. The effect of porosity on wettability, in fact, overcome the one induced by surface roughness increases [54–56]. Considering that, it is important to underline that the value obtained during WCA test are distorted by liquid capillary transport effect and shouldn't be considered as an increase of hydrophilicity. In addition, in PEO-B systems lower WCA value (if compared to PEO-A ones) are obtained due to the already commented differences in porous structure between PEO-A (smaller pores) and PEO-B (larger pores).

Mechanical Properties

To evaluate different mechanical performance of the membranes, elastic modulus (E), tensile strength (TS) and elongation at break (EB) have been measured and results are reported in Table 3.

PLA exhibits elastic modulus, tensile strength and elongation at break of 60 MPa, 1.2 MPa and 45% respectively. If compared to PLA, all the unleached systems containing PEO-A does not show substantial differences i.e. mechanical performance that is controlled by PLA. These results are in accordance with other similar systems [40]. On the contrary, PEO-B membrane shows a different behavior: as PEO-B content increase mechanical performance of the samples decrease. In detail, the addition of 25%, 50% and 75% of PEO-B induced a remarkable decrease in elastic modulus of PLA/PEO-B25, PLA/PEO-B50 and PLA/PEO-B75. If compared to the corresponding non-leached systems, PLA/

Table 2 FTIR peak values and relative functional groups

Polymer	Wavenumber (cm^{-1})	Functional group	Vibrations	Reference
PLA	1759	–C=O	Carbonyl stretch	[45, 46]
PEO	1344	CH2	Symmetric stretching	[47–49]
PEO	1150	C–O–C	Stretching vibration	[47–49]
PEO	2891	CH	Stretching mode	[47–49]

Table 3 Elastic modulus (E), tensile strength (TS), and elongation at break (EB) of the electrospun membranes

Sample	E (MPa)	TS (MPa)	EB (%)
PLA	60 ± 2.3	1.2 ± 0.5	45 ± 4.6
PLA/PEO-A25	58 ± 3.7	2.0 ± 0.4	56 ± 7.2
PLA/PEO-A50	62 ± 12.8	0.9 ± 0.3	48 ± 9.5
PLA/PEO-A75	57 ± 7.7	0.8 ± 0.3	43 ± 5.6
PLA/PEO-B25	44 ± 0.2	1.4 ± 0.1	54 ± 13.9
PLA/PEO-B50	26 ± 11.2	0.1 ± 0.1	42 ± 9.2
PLA/PEO-B75	12 ± 3.5	0.4 ± 0.2	26 ± 13.1
PLA/PEO-A25W	52 ± 8.5	0.8 ± 0.2	45 ± 6.5
PLA/PEO-B25W	10 ± 2.1	0.5 ± 0.4	18 ± 3.1
PLA/PEO-A25L	55 ± 5.0	1.8 ± 0.6	38 ± 11.0
PLA/PEO-B25L	12 ± 2.0	0.5 ± 0.9	15 ± 6.0

PEO-A25W exhibits similar mechanical properties, on the contrary, PLA/PEO-B25W shows a clear decrease in E, TS and EB. PLA/PEOA-25L and PLA/PEO-B25L (DS) showed the same behavior of their SS counterparts. The simultaneous decrease in modulus and elongation at break on increasing PEO-B content, confirms the typical behavior of immiscible couples. In fact, poor miscibility of PEO-B phase leads to the formation of an irregular and heterogeneous fibrous structure with consequent disruption of some fibers. According to the morphological analysis, moreover, the presence of PEO-B phase agglomerations along the fibers induces discontinuity in the membranes structure leading to the formation of weak points across them. On the contrary, the good miscibility of PEO-A in PLA allows obtaining homogeneous structures leading to better mechanical performance if compare with PEO-B systems [40].

## Oil Spill Clean-up Capacity of the Porous Membranes

The particular architecture observed for these membranes suggests their potential use as sorbent materials for oil spill cleanup. Six different kinds of oils (motor oil, exhausted motor oil, olive oil, exhausted olive oil, sunflower oil and exhausted sunflower oil) were chosen and their adsorption capacity by PLA, PLA/PEO-A25L, PLA/PEO-B25L, PLA/PEO-A25W and PLA/PEO-B25W were teste and results are shown in Fig. 10. As expected, PLA membranes showed the lowest q value for all kind of oils tested. DS leached systems showed a slight increase in absorption capacity if compared to PLA membrane. The maximum absorption capacity for every type of oil was achieved by one-step leached systems. In particular, PLA/PEO-A25W and PLA/PEO-B25W showed the highest oil adsorption capacity for exhausted motor oil, with a q value of 115 and 137 g/g respectively. According to the scientific literature, the presence of high porosity, high surface area or empty channels increase oil absorption capacity of a membrane [6, 57]. The low q value of PLA membrane, in fact, could be likely ascribed to its smooth and homogeneous fibers. The increase in absorption capacity values displayed by DS systems, could be reasonably attributed to the presence of fibers with porous surfaces. The best q values displayed by PLA/PEO-A25W and PLA/PEO-B25W are could be likely ascribed to the combination of a shell with large pores (also structured in furrows) and a core hollow structure. This particular structure, in fact, likely caused an increase of surface area and the formation of channels facilitated a deeper penetration of motor oil in the whole membrane.

Moreover, PLA/PEO-A25W and PLA/PEO-B25W exhibit the best adsorption capacities for motor oil and the worst adsorption capacities for sunflower oil. According to the scientific literature, this behavior should be addressed to the higher viscosity of motor oil (if compared to olive and sunflower oil ones) that make it difficult for the oil to flow out of the membranes once it enters the channels of the hollow fibers [6].

In Movie S1 and Fig. 11 is reported the oil spill cleanup process successfully carried out by PLA/PEO-B25W.

Fig. 10 Oil adsorption capacities of motor oil, exhausted motor oil, olive oil, exhausted olive oil, sunflower oil and exhausted sunflower oil by membranes
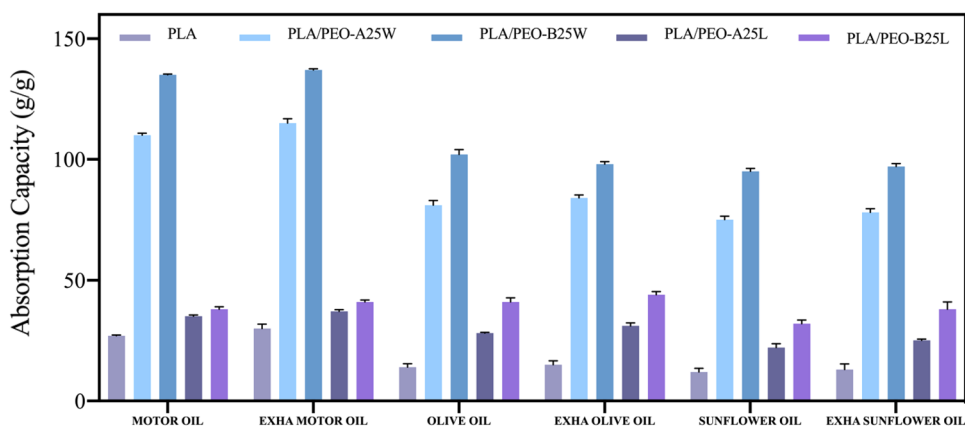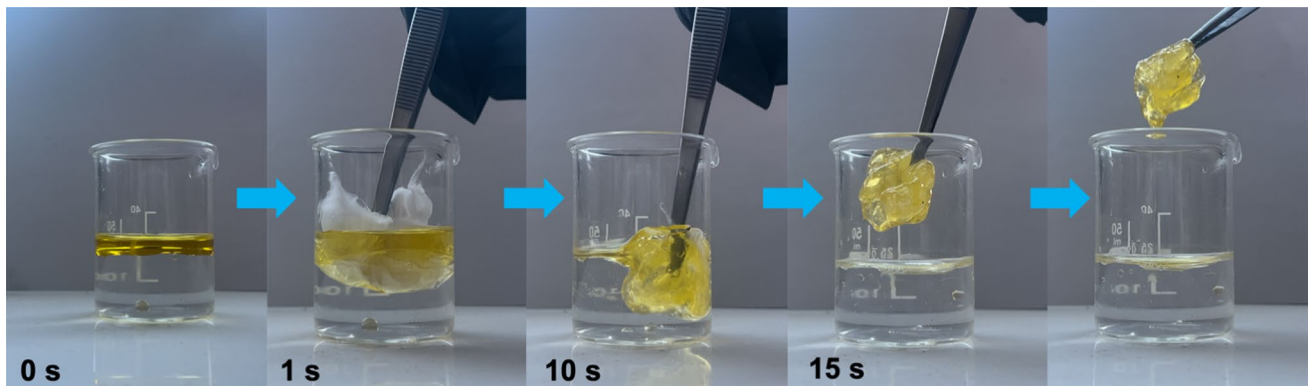
Fig. 11 Olive oil spill clean-up process using PLA/PEO-B25W

Table 4 Comparison of oil adsorption abilities between wet coaxial electrospun PLA/PEO membrane and other adsorbents systems reported in literature

Membrane	Materials	Additional chemicals	Processing	Absorption capacity [g/g]	Reference
Coaxial and hollow fibers	PAN, PMMA	Acetone, chloroform	Electrospinning + stabilization + carbonization	10–45	[58]
Porous fibers	PLA	–	Electrospinning + annealing for 12 h	22–42	[59]
Rough nanofibers	PLA, PHB	–	Electrospinning	10–15	[60]
Rough nanofibers	PLA, SiO2	–	Solution blow spinning	20	[61]
Fibers and micro spheres	PCL, MSO	–	Electrospinning + electrospray	22–32	[62]
Fibers and micro spheres	PMMA, PDMS	Hexane, curing agent	Electrospinning + electrospray + curing 3 h	55–40	[14]
Coaxial and hollow fibers	PLA, PDLA	n-eptan	Electrospinning + leaching-two steps	90–200	[6]
Coaxial and hollow fibers	PLA, PVA	–	Electrospinning + leaching-two steps	23	[25]
Coaxial and porous hollow fibers	PLA, PEO	–	One step electrospinning and leaching	70–137	this work

The same representative steps for pure PLA-based membranes were shown in Fig. S7 for comparison.

Table 4 shows the oil adsorption capacities of the wet coaxial electrospun PLA/PEO membranes and other adsorbents reported in literature. It can be noticed that, compared to other similar systems, wet coaxial electrospun PLA/PEO membranes exhibited excellent oil absorption capacity. Moreover, devices produced in this work were obtained in a single step process without using any additional chemicals.

Reusability of the Porous Membranes

Exhausted motor oil absorption ability of the electrospun membranes was monitored for up to five cycles to evaluate their reusability and the related performance. In this direction, membranes were washed in ethanol after used and the re-exposed to oil. The results are shown in Fig. 12.

After each cycle, PLA showed a decrease in absorption capacity (q). This decrease in q is probably attributable to the incomplete removal of oil from the membrane between cycles due to difficulty of penetration of the solvent during the rinsing phases.

A slight decrease (statistically significant only from the III cycle onwards) in q can be also observed for PLA/PEO-B25W after each cycle due to partial macroscopical damage of the membrane during the rinsing phase. On the contrary, no substantial variations can be evidenced for DS leached systems even after five cycle of oil absorption. The same behaviour can be observed for PLA/PEO-A25W and, again, is probably attributable to the peculiar fibers structure achieved for this system. During the rinsing phases, in fact, the penetration of the solvent is promoted by the porous and hollow structure of the fibers [14], thus granting a complete oil removal.

Conclusion

In this work, a new method for produce, in one-step, biodegradable membranes with hollow and porous fibers with high oil absorbance efficiency is presented. More in detail,

Fig. 12 Exhausted motor oil absorption capacity monitored for up to 5 cycles for PLA, PLA/PEO-A25W, PLA/PEO-B25W, PLA/PEO-A25L, PLA/PEO-B25L
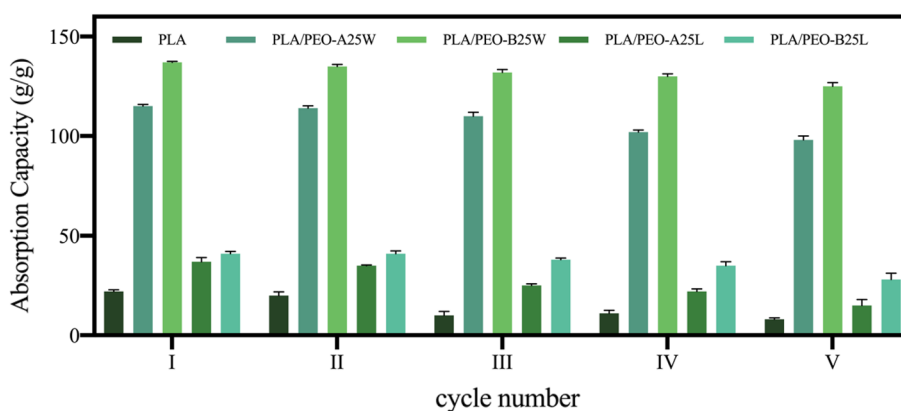
membranes with hollow and (or) porous and fibers, based on polylactic acid (PLA) and polyethylene oxide (PEO) blends, were prepared using two approaches: (i) conventional coaxial electrospinning followed by leaching treatment (double-step); (ii) coaxial wet electrospinning with in situ leaching (single-step). The relationships between materials, process, properties and structure of the obtained devices were analysed trough rheological, morphological, mechanical and surface characterizations. Results reveal that by varying PEO molecular weight and amount in the PLA/PEO blends it was possible to tune the fibers structure, especially after the leaching treatment, due to the difference in miscibility of the phases. Moreover, wet electrospinning production method allowed fabricating hollow and porous fibers (i.e. shell and core leaching) which, otherwise, could not be obtained with the double-step process that only leads to surface porosity (i.e. shell leaching). In fact, during the in situ leaching, not jet stabilized fibers, containing residual solvent, come into contact with the leaching agent promoting its penetration into the core creating the hollow structure.

Differences in polymeric compositions or morphology have led also to a variation in membranes mechanical performance: the occurrence of discontinuity in the fibers, due to the presence of an immiscible phase or porosity, leads to a decrease of membranes elastic modulus.

The two-step and the in situ leached systems both displayed morphological characteristics and mechanical property potentially suitable for oil spill cleanup application. Oil absorbance test reveal that membranes obtained via single-step method displayed higher performance in oil removal, if compared to the ones obtained through the post processing leaching, due to their hollow and porous structure that ensure higher exposed surface area.

Supplementary Information The online version contains supplementary material available at https://doi.org/10.1007/s10924-023-02876-0.

Author Contributions RS: Conceptualization, Methodology, Validation, Resources, Data Curation, Writing -Review & Editing, Supervision, Project Administration, Funding Acquisition.EFG: Methodology, Software, Validation, Formal Analysis, Investigation, Data Curation, Writing - Original Draft, Writing -Review & Editing, Visualization. MCC: Methodology, Software, Validation, Formal Analysis, Investigation, Data Curation, Writing - Original Draft, Writing -Review & Editing, Visualization.

Data Availability The data presented in this study are available on request from the corresponding authors.

Declarations

Conflict of interest The authors declare no conflict of interest.

References

1. Isık T, Demir MM (2018) Tailored electrospun fibers from waste polystyrene for high oil adsorption. Sustain Mater Technol 18:e00084. https://doi.org/10.1016/J.SUSMAT.2018.E00084

2. Sankaranarayanan S, Lakshmi DS, Vivekanandhan S, Ngamcharussrivichai C (2021) Biocarbons as emerging and sustainable hydrophobic/oleophilic sorbent materials for oil/water separation. Sustain Mater Technol 28:e00268. https://doi.org/10.1016/J.SUSMAT.2021.E00268

3. Lin H, Chen K, Zheng S, Zeng R, Lin Y, Jian R, Bai W, Xu Y (2022) Facile fabrication of natural superhydrophobic eleostearic acid-SiO2@cotton fabric for efficient separation of oil/water mixtures and emulsions. Sustain Mater Technol 32:e00418. https://doi.org/10.1016/J.SUSMAT.2022.E00418

4. Sadler E, Crick CR (2021) Suction or gravity-fed oil-water separation using PDMS-coated glass filters. Sustain Mater Technol 29:e00321. https://doi.org/10.1016/J.SUSMAT.2021.E00321

5. Shi C, Chen Y, Yu Z, Li S, Chan H, Sun S, Chen G, He M, Tian J (2021) Sustainable and superhydrophobic spent coffee ground-derived holocellulose nanofibers foam for continuous oil/water separation. Sustain Mater Technol 28:e00277. https://doi.org/10.1016/J.SUSMAT.2021.E00277

6. Fan Deng Y, Zhang N, Huang T, Zhou Lei Y, Wang Y (2022) Constructing tubular/porous structures toward highly efficient oil/water separation in electrospun stereocomplex polylactide fibers via coaxial electrospinning technology. Appl Surf Sci 573:151619. https://doi.org/10.1016/J.APSUSC.2021.151619

7. Gulino EF, Citarrella MC, Maio A, Scaffaro R (2022) An innovative route to prepare in situ graded crosslinked PVA graphene

electrospun mats for drug release. Compos Part A Appl Sci Manuf 155:106827. https://doi.org/10.1016/J.COMPOSITESA.2022.106827

8. He T, Wang J, Huang P, Zeng B, Li H, Cao Q, Zhang S, Luo Z, Deng DYB, Zhang H, Zhou W (2015) Electrospinning polyvinylidene fluoride fibrous membranes containing anti-bacterial drugs used as wound dressing. Colloids Surf B Biointerfaces 130:278–286. https://doi.org/10.1016/J.COLSURFB.2015.04.026

9. Yang D, Li Y, Nie J (2007) Preparation of gelatin/PVA nanofibers and their potential application in controlled release of drugs. Carbohydr Polym 69:538–543. https://doi.org/10.1016/J.CARBPOL.2007.01.008

10. Sarbatly R, Krishnaiah D, Kamin Z (2016) A review of polymer nanofibres by electrospinning and their application in oil–water separation for cleaning up marine oil spills. Mar Pollut Bull 106:8–16. https://doi.org/10.1016/J.MARPOLBUL.2016.03.037

11. Zhang L, Narita C, Himeda Y, Honma H, Yamada K (2022) Development of highly oil-absorbent polylactic-acid microfibers with a nanoporous structure via simple one-step centrifugal spinning. Sep Purif Technol. https://doi.org/10.1016/j.seppur.2021.120156

12. Scaffaro R, Lopresti F, Catania V, Santisi S, Cappello S, Botta L, Quatrini P (2017) Polycaprolactone-based scaffold for oil-selective sorption and improvement of bacteria activity for bioremediation of polluted water: porous PCL system obtained by leaching melt mixed PCL/PEG/NaCl composites: oil uptake performance and bioremediation efficiency. Eur Polym J 91:260–273. https://doi.org/10.1016/J.EURPOLYMJ.2017.04.015

13. Wang X, Yu J, Sun G, Ding B (2016) Electrospun nanofibrous materials: a versatile medium for effective oil/water separation. Mater Today 19:403–414. https://doi.org/10.1016/J.MATTOD.2015.11.010

14. Gao J, Song X, Huang X, Wang L, Li B, Xue H (2018) Facile preparation of polymer microspheres and fibers with a hollow core and porous shell for oil adsorption and oil/water separation. Appl Surf Sci 439:394–404. https://doi.org/10.1016/J.APSUSC.2018.01.013

15. Liu M, Duan XP, Li YM, Yang DP, Long YZ (2017) Electrospun nanofibers for wound healing. Mater Sci Eng, C 76:1413–1423. https://doi.org/10.1016/J.MSEC.2017.03.034

16. Massarelli E, Silva D, Pimenta AFR, Fernandes AI, Mata JLG, Armês H, Salema-Oom M, Saramago B, Serro AP (2021) Polyvinyl alcohol/chitosan wound dressings loaded with antiseptics. Int J Pharm. https://doi.org/10.1016/j.ijpharm.2020.120110

17. Liu X, Lin T, Fang J, Yao G, Zhao H, Dodson M, Wang X (2010) In vivo wound healing and antibacterial performances of electrospun nanofibre membranes. J Biomed Mater Res A 94A:499–508. https://doi.org/10.1002/JBM.A.32718

18. Li TT, Zhong Y, Peng HK, Ren HT, Chen H, Lin JH, Lou CW (2021) Multiscale composite nanofiber membranes with asymmetric wetability: preparation, characterization, and applications in wound dressings. J Mater Sci 56:4407–4419. https://doi.org/10.1007/s10853-020-05531-4

19. Scaffaro R, Settanni L, Gulino EF (2023) Release profiles of carvacrol or chlorhexidine of PLA/graphene nanoplatelets membranes prepared using electrospinning and solution blow spinning: a comparative study. Molecules 28:1967. https://doi.org/10.3390/MOLECULES28041967

20. Yoon J, Yang HS, Lee BS, Yu WR (2018) Recent progress in coaxial electrospinning: new parameters, various structures, and wide applications. Adv Mater 30:1704765. https://doi.org/10.1002/ADMA.201704765

21. Maio A, Gammino M, Gulino EF, Megna B, Fara P, Scaffaro R (2020) Rapid one-step fabrication of graphene oxide-decorated polycaprolactone three-dimensional templates for water treatment.

ACS Appl Polym Mater 2:4993–5005. https://doi.org/10.1021/ACSAPM.0C00852/ASSET/IMAGES/LARGE/AP0C00852_0010.JPEG

22. Sofi HS, Ashraf R, Khan AH, Beigh MA, Majeed S, Sheikh FA (2019) Reconstructing nanofibers from natural polymers using surface functionalization approaches for applications in tissue engineering, drug delivery and biosensing devices. Mater Sci Eng, C 94:1102–1124. https://doi.org/10.1016/J.MSEC.2018.10.069

23. Wang X, Min M, Liu Z, Yang Y, Zhou Z, Zhu M, Chen Y, Hsiao BS (2011) Poly(ethyleneimine) nanofibrous affinity membrane fabricated via one step wet-electrospinning from poly(vinyl alcohol)-doped poly(ethyleneimine) solution system and its application. J Memb Sci 379:191–199. https://doi.org/10.1016/J.MEMSCI.2011.05.065

24. Zhang B, Lu C, Liu Y, Zhou P (2018) Wet spun polyacrylonitrile-based hollow fibers by blending with alkali lignin. Polymer (Guildf) 149:294–304. https://doi.org/10.1016/J.POLYMER.2018.07.019

25. Jiang AY, Pan ZJ (2020) Cross-sectional porosity and oil sorption of PLA nanofibers with hollow and lotus root-like structures. J Fiber Bioeng Info 13:51–60. https://doi.org/10.3993/jfbim00335

26. Song P, Zhou C, Fan H, Zhang B, Pei X, Fan Y, Jiang Q, Bao R, Yang Q, Dong Z, Zhang X (2018) Novel 3D porous biocomposite scaffolds fabricated by fused deposition modeling and gas foaming combined technology. Compos B Eng 152:151–159. https://doi.org/10.1016/j.compositesb.2018.06.029

27. Hou Q, Grijpma DW, Feijen J (2003) Porous polymeric structures for tissue engineering prepared by a coagulation, compression moulding and salt leaching technique. Biomaterials 24:1937–1947. https://doi.org/10.1016/S0142-9612(02)00562-8

28. Kim TG, Chung HJ, Park TG (2008) Macroporous and nanofibrous hyaluronic acid/collagen hybrid scaffold fabricated by concurrent electrospinning and deposition/leaching of salt particles. Acta Biomater 4:1611–1619. https://doi.org/10.1016/J.ACTBIO.2008.06.008

29. Zhang YZ, Feng Y, Huang ZM, Ramakrishna S, Lim CT (2006) Fabrication of porous electrospun nanofibres. Nanotechnology 17:901. https://doi.org/10.1088/0957-4484/17/3/047

30. Ning J, Zhang X, Yang H, Xu ZL, Wei YM (2016) Preparation of porous PVDF nanofiber coated with Ag NPs for photocatalysis application. Fibers Polym 17:21–29. https://doi.org/10.1007/S12221-016-5705-7/METRICS

31. Sorze A, Valentini F, Dorigato A, Pegoretti A (2021) Salt leaching as a green method for the production of polyethylene foams for thermal energy storage applications. Polym Eng Sci. https://doi.org/10.21203/rs.3.rs-680156/v1

32. Pi HJ, Liu XX, Liao JY, Zhou YY, Meng C (2022) Lightweight polyethylene/hexagonal boron nitride hybrid thermal conductor fabricated by melt compounding plus salt leaching. Polymers (Basel) 14:852. https://doi.org/10.3390/POLYM14050852

33. Scaffaro R, Lopresti F, Botta L, Rigoglioso S, Ghersi G (2016) Melt processed PCL/PEG scaffold with discrete pore size gradient for selective cellular infiltration. Macromol Mater Eng 301:182–190. https://doi.org/10.1002/MAME.201500289

34. Ryan J, Dizon C, Catherine C, Gache L, Mae H, Cascolan S, Cancino LT, Advincula RC (2021) Post-processing of 3D-printed polymers. Technologies 9:61. https://doi.org/10.3390/TECHNOLOGIES9030061

35. Yu X, Xiang H, Long Y, Zhao N, Zhang X, Xu J (2010) Preparation of porous polyacrylonitrile fibers by electrospinning a ternary system of PAN/DMF/H2O. Mater Lett 64:2407–2409. https://doi.org/10.1016/J.MATLET.2010.08.006

36. Guillen GR, Pan Y, Li M, Hoek EMV (2011) Preparation and characterization of membranes formed by nonsolvent induced

phase separation: a review. Ind Eng Chem Res 50:3798–3817. https://doi.org/10.1021/IE101928R

37. Nakanishi K, Tanaka N (2007) Sol-gel with phase separation hierarchically porous materials optimized for high-performance liquid chromatography separations. Acc Chem Res 40:863–873. https://doi.org/10.1021/AR600034P

38. Scaffaro R, Lopresti F (2018) Processing, structure, property relationships and release kinetics of electrospun PLA/Carvacrol membranes. Eur Polym J 100:165–171. https://doi.org/10.1016/J.EURPOLYMJ.2018.01.035

39. Wei X, Cai J, Lin S, Li F, Tian F (2021) Controlled release of monodisperse silver nanoparticles via in situ cross-linked polyvinyl alcohol as benign and antibacterial electrospun nanofibers. Colloids Surf B Biointerfaces 197:111370. https://doi.org/10.1016/J.COLSURFB.2020.111370

40. Scaffaro R, Gulino FE, Lopresti F (2018) Structure–property relationship and controlled drug release from multiphasic electrospun carvacrol-embedded polylactic acid/polyethylene glycol and polylactic acid/polyethylene oxide nanofiber mats. J Ind Text 49:943–966. https://doi.org/10.1177/1528083718801359

41. Xu Y, Guo P, Akono AT (2022) Novel wet electrospinning inside a reactive pre-ceramic gel to yield advanced nanofiber-reinforced geopolymer composites. Polymers (Basel) 14:3943. https://doi.org/10.3390/POLYM14193943/S1

42. Doshi J, Reneker DH (1995) Electrospinning process and applications of electrospun fibers. J Electrostat 35:151–160. https://doi.org/10.1016/0304-3886(95)00041-8

43. Scaffaro R, Lo Re G, Rigoglioso S, Ghersi G (2012) 3D polylactide-based scaffolds for studying human hepatocarcinoma processes in vitro. Sci Technol Adv Mater 13:12. https://doi.org/10.1088/1468-6996/13/4/045003

44. Zhou Y, Tan GZ, Zhou Y, Tan GZ (2020) Core-sheath wet electrospinning of nanoporous polycaprolactone microtubes to mimic fenestrated capillaries. Macromol Mater Eng 305:2000180. https://doi.org/10.1002/MAME.202000180

45. Farkas NI, Marincaş L, Barabás R, Bizo L, Ilea A, Turdean GL, Toşa M, Cadar O, Barbu-Tudoran L (2022) Preparation and characterization of doxycycline-loaded electrospun PLA/HAP nanofibers as a drug delivery system. Materials 15:2105. https://doi.org/10.3390/MA15062105

46. Ghafari R, Scaffaro R, Maio A, Gulino EF, Lo Re G, Jonoobi M (2020) Processing-structure-property relationships of electrospun PLA-PEO membranes reinforced with enzymatic cellulose nanofibers. Polym Test 81:106182. https://doi.org/10.1016/j.polymertesting.2019.106182

47. Darbasizadeh B, Mortazavi SA, Kobarfard F, Jaafari MR, Hashemi A, Farhadnejad H, Feyzi-barnaji B (2021) Electrospun Doxorubicin-loaded PEO/PCL core/sheath nanofibers for chemopreventive action against breast cancer cells. J Drug Deliv Sci Technol. 64:102576. https://doi.org/10.1016/J.JDDST.2021.102576

48. Melda Eskitoros-Togay Ş, Bulbul YE, Tort S, Demirtaş Korkmaz F, Acartürk F, Dilsiz N (2019) Fabrication of doxycycline-loaded electrospun PCL/PEO membranes for a potential drug delivery system. Int J Pharm. https://doi.org/10.1016/j.ijpharm.2019.04.073

49. Goettems Kuntzler S, Vieira Costa JA, Greque De Morais M (2018) Development of electrospun nanofibers containing chitosan/PEO blend and phenolic compounds with antibacterial activity. Int J Biol Macromol. https://doi.org/10.1016/j.ijbiomac.2018.05.224

50. Li S, Molina I, Bueno Martinez M, Vert M (2002) Hydrolytic and enzymatic degradations of physically crosslinked hydrogels prepared from PLA/PEO/PLA triblock copolymers. J Mater Sci Mater Med 13:81–86. https://doi.org/10.1023/A:1013651022431/METRICS

51. Valente TAM, Silva DM, Gomes PS, Fernandes MH, Santos JD, Sencadas V (2016) Effect of sterilization methods on electrospun poly(lactic acid) (PLA) fiber alignment for biomedical applications. ACS Appl Mater Interfaces 8:3241–3249. https://doi.org/10.1021/ACSAMI.5B10869/ASSET/IMAGES/ACSAMI.5B10869.SOCIAL.JPEG_V03

52. Abudula T, Saeed U, Memic A, Gauthaman K, Hussain MA, Al-Turaif H (2019) Electrospun cellulose Nano fibril reinforced PLA/PBS composite scaffold for vascular tissue engineering. J Polym Res 26:1–15. https://doi.org/10.1007/S10965-019-1772-Y/FIGURES/11

53. Moradkhannejhad L, Abdouss M, Nikfarjam N, Shahriari MH, Heidary V (2020) The effect of molecular weight and content of PEG on in vitro drug release of electrospun curcumin loaded PLA/PEG nanofibers. J Drug Deliv Sci Technol. 56:101554. https://doi.org/10.1016/J.JDDST.2020.101554

54. Scaffaro R, Citarrella MC, Gulino EF (2022) Opuntia Ficus Indica based green composites for NPK fertilizer controlled release produced by compression molding and fused deposition modeling. Compos Part A Appl Sci Manuf 159:107030. https://doi.org/10.1016/J.COMPOSITESA.2022.107030

55. Mehrvarz A, Khalil-Allafi J, Etminanfar M, Mahdavi S (2021) The study of morphological evolution, biocorrosion resistance, and bioactivity of pulse electrochemically deposited Hydroxyapatite/ZnO composite on NiTi superelastic alloy. Surf Coat Technol 423:127628. https://doi.org/10.1016/J.SURFCOAT.2021.127628

56. Xiong B, Li J, He C, Tang X, Lv Z, Li X, Yan X (2020) Effect of pore morphology and surface roughness on wettability of porous titania films. Mater Res Exp. 7:115013. https://doi.org/10.1088/2053-1591/ABC770

57. Lin J, Shang Y, Ding B, Yang J, Yu J, Al-Deyab SS (2012) Nanoporous polystyrene fibers for oil spill cleanup. Mar Pollut Bull 64:347–352. https://doi.org/10.1016/J.MARPOLBUL.2011.11.002

58. Mantripragada S, Gbewonyo S, Deng D, Zhang L (2020) Oil absorption capability of electrospun carbon nanofibrous membranes having porous and hollow nanostructures. Mater Lett 262:127069. https://doi.org/10.1016/J.MATLET.2019.127069

59. Liang JW, Prasad G, Wang SC, Wu JL, Lu SG (2019) Enhancement of the oil absorption capacity of poly(lactic acid) nano porous fibrous membranes derived via a facile electrospinning method. Appl Sci 9:1014. https://doi.org/10.3390/APP9051014

60. Yeo JCC, Kai D, Teng CP, Lin EMJR, Tan BH, Li Z, He C (2020) Highly washable and reusable green nanofibrous sorbent with superoleophilicity biodegradability, and mechanical robustness. ACS Appl Polym Mater 2:4825–4835. https://doi.org/10.1021/ACSAPM.0C00786

61. Ye B, Jia C, Li Z, Li L, Zhao Q, Wang J, Wu H (2020) Solution-blow spun PLA/SiO2 nanofiber membranes toward high efficiency oil/water separation. J Appl Polym Sci 137:49103. https://doi.org/10.1002/APP.49103

62. Zhang G, Wang P, Zhang X, Xiang C, Li L (2019) Preparation of hierarchically structured PCL superhydrophobic membrane via alternate electrospinning/electrospraying techniques. J Polym Sci B Polym Phys 57:421–430. https://doi.org/10.1002/POLB.24795

Authors and Affiliations

Roberto Scaffaro[1] · **Emmanuel Fortunato Gulino[1]** · **Maria Clara Citarrella[1]**

✉ Roberto Scaffaro
roberto.scaffaro@unipa.it

✉ Emmanuel Fortunato Gulino
emmanuelfortunato.gulino@unipa.it

Maria Clara Citarrella
mariaclara.citarrella@unipa.it

[1] Department of Engineering, University of Palermo, Viale Delle Scienze, ed. 6, 90128 Palermo, PA, Italy